Photophysical and Electrochemical Properties of New Bacteriochlorins and Characterization of Radical Cation and Radical Anion Species

Shunichi Fukuzumi,*,† Kei Ohkubo,† Yihui Chen,‡ Ravindra K. Pandey,*,‡,§ Riqiang Zhan,# Jianguo Shao,# and Karl M. Kadish*,#

Department of Material and Life Science, Graduated School of Engineering, Osaka University, CREST, Japan Science and Technology Corporation (JST), 2-1 Yamada-oka, Suita, Osaka 565-0871, Japan, Chemistry Division, Photodynamic Therapy Center, Roswell Park Cancer Institute, Buffalo, New York 14263, Department of Nuclear Medicine, Roswell Park Cancer Institute, Buffalo, New York 14263, and Department of Chemistry, University of Houston, Houston, Texas 77204-5003

Received: February 19, 2002

The synthesis, photophysical, and photochemical properties of a series of stable bacteriochlorins containing a fused six-member anhydride or an imide ring are discussed. The Q_y band ($a_{1u} \rightarrow e_{gx}$ transition) in the near-infrared region (NIR) lies between 788 and 831 nm depending upon the macrocycle substituents. Compounds with such a long-wavelength absorption are highly promising for their potential use in photodynamic therapy. Fluorescence maxima are also observed in the long-wavelength region of the spectrum, between 804 and 842 nm, and have lifetimes between 1.1 and 1.4 ns. The phosphorescence maxima are red-shifted to 840−870 nm. The triplet−triplet transient absorption spectra are observed to have maxima between 570 and 640 nm with lifetimes between 72 and 150 μs. The triplet excited states are efficiently quenched by oxygen to produce singlet oxygen. The quantum yields of the generated singlet oxygen were determined to be in the range of 0.33−0.55. The bacteriochlorin derivatives are easy to oxidize by one electron, and reversible half-wave potentials range between 0.65 and 0.82 V vs SCE in benzonitrile containing 0.1 M tetra-*n*-butylammonium perchlorate (TBAP). The second oxidation is irreversible and occurs at a rather constant potential of 1.17−1.22 V independent of the macrocycle substituents. The bacteriochlorin derivatives are also easy to reduce, and the reversible first and second one-electron reduction potentials range between −0.53 and −0.80 V and between −0.95 and −1.28 V vs SCE, respectively. Spectroelectrochemical measurements reveal the expected π radical cation and π radical anion marker bands of the bacteriochlorin derivatives. The electron spin resonance (ESR) spectra of the radical cations and radical anions produced by the chemical oxidation and reduction are reported, and the experimental and calculated spin densities are compared to each other.

Introduction

Porphyrin-based photosensitizers have been the subject of enormous interest because of their potential use in photodynamic therapy (PDT).[1] The major drawback associated with porphyrin-based photosensitizers is related to their weak absorption in the long-wavelength region of the spectrum. It has been well-established that both absorption and scattering of light by tissue increases as the wavelength decreases.[1] Heme proteins in tissue account for most of the tissue-related absorption of light in the visible region. Light penetration drops off rapidly below 550 nm, but it doubles from 550 to 630 nm and doubles again upon going to 700 nm.[1] The light penetration in tissue is further increased as the wavelength moves toward 800 nm. Thus, the most efficient sensitizers are those that have strong absorption bands above 800 nm.[2]

Porphyrins, chlorins, and bacteriochlorins have a different π electron conjugation. The number of reduced double bonds in the pyrrole rings is zero in the case of porphyrins, one in the case of chlorins and two in the case of bacteriochlorins. This difference in the degree of macrocycle conjugation causes a considerable change in the excited states, absorption spectra, and redox properties.[3,4] The ionization potentials of the tetrapyrroles decrease with increasing peripheral saturation,[5] consistent with the electrochemical data.[6] Such a decrease in the HOMO energy results in a red shift of the absorption band of the first excited state (Q_x) and an increase in its intensity.[3,7] This is the reason one emphasis on the development of new antitumor drugs has focused on chlorin- and bacteriochlorin-related compounds.[8,9] Such reduced macrocycles are also central to many processes of biological significance such as in photosynthesis.[10,11]

To investigate the effect of overall lipophilicity in photosensitizing efficacy, starting from chlorophyll, a number of new photosensitizers have been synthesized in recent years by introducing various type of substituents at the peripheral position of the molecule.[1,12−14] Interestingly, it has also been shown that the five-member isocyclic ring present in chlorophyll *a* can be converted into a fused six-member anhydride, an isoimide, or an imide ring.[1] The position of such fused ring systems extends their long-wavelength absorptions from 660 to 700 nm.[1] Among

* To whom correspondence should be addressed. E-mail addresses: fukuzumi@ap.chem.eng.osaka-u.ac.jp, Ravindra.Pandey@RoswellPark.org, KKadish@uh.edu.
† Osaka University.
‡ Photodynamic Therapy Center, Roswell Park Cancer Institute.
§ Department of Nuclear Medicine, Roswell Park Cancer Institute.
# University of Houston.

10.1021/jp025665x CCC: $22.00
Published on Web 04/18/2002

these porphyrin-based analogues, compounds containing the six-member imide ring were found to be more stable in vivo that those bearing a fused anhydride or isoimide ring system.[1]

For developing photosensitizers with long-wavelength absorption near 800 nm, several naturally occurring bacteriochlorins have been evaluated for their use in PDT.[15] Unfortunately, these compounds were found to be extremely sensitive to oxidation, which results in a rapid transformation into a mixture of chlorins. These metabolite(s) generally have an absorption maxima at or below 660 nm. Furthermore, if a laser is used to excite the bacteriochlorin in vivo, oxidation may result in the formation of new chromophores outside the laser window, thus reducing the photosensitizing efficacy. Therefore, there has been an increasing interest in the synthesis of stable bacteriochlorins, either from bacteriochlorophyll *a* or by modifying the form of the porphyrin/chlorin system.[1]

The photophysical and electrochemical properties, which are given important consideration in designing improved photosensitizers, may also be altered by modifying the chlorin or bacteriochlorin with specific substituents.[16] Although the visible absorption spectra of porphyrins, chlorins, and bacteriochlorins are well-known,[17] limited information is available about the absorption and electron spin resonance (ESR) spectra of the one-electron oxidized or one-electron reduced chlorin- or bacteriochlorin compounds.[18−22] In addition, the effect of substituents on the photophysical or electrochemical properties of chlorins or bacteriochlorins has yet to be examined.

We report herein the synthesis of a series of stable bacteriochlorins containing a fused anhydride or imide ring and examine the effects of these modifications on their photophysical and electrochemical properties. The newly synthesized compounds exhibit long-wavelength absorptions in the near-infrared (NIR) region of the spectrum with the value being between 788 and 831 nm depending on the macrocyclic substituents and are thus promising candidates for use in photodynamic therapy. Photoexcitation of the NIR bands of these compounds in the presence of oxygen results in the efficient formation of singlet oxygen. UV−visible and ESR spectra of the one-electron oxidized and one-electron reduced bacteriochlorin derivatives are of significant interest as intermediates in photosynthesis[23] and are also characterized in this study.

Experimental Section

Materials. Naphthalene radical anion was prepared by reduction of naphthalene by sodium in THF. Tris(2,2′-bipyridyl)-ruthenium dichloride hexahydrate, $[Ru(bpy)_3]Cl_2 \cdot 6H_2O$ was obtained commercially from Aldrich. The oxidation of $[Ru(bpy)_3]Cl_2$ with lead dioxide in aqueous H_2SO_4 gives $[Ru(bpy)_3]^{3+}$, which is isolated as the PF_6^- salt, $[Ru(bpy)_3](PF_6)_3$.[24] Tetra-*n*-butylammonium perchlorate (TBAP), used as a supporting electrolyte for the electrochemical measurements, was obtained from Fluka Fine Chemical, recrystallized from ethanol, and dried in vacuo prior to use. Benzonitrile was purchased from Wako Pure Chemical Ind., Ltd. and purified by successive distillation over P_2O_5.[25] Benzene-d_6 (C_6D_6), used as solvent, was obtained from EURI SO-TOP, France, and used without further purification.

Instrumentation. Melting points were determined in a hot-plate melting-point apparatus and are uncorrected. ^{1}H NMR spectra were recorded in $CDCl_3$ at 400 MHz with TMS as an internal standard. E. Merck silica gel for column chromatography and E. Merck precoated TLC plates, silica gel F_{254}, for preparative thin-layer chromatography were used. The electronic absorption spectra were taken with a Varian Gary 50 Bio UV−visible spectrophotometer using dichloromethane as a solvent.

Synthesis of Bacteriochlorins. *3-Acetyl-bacteriopurpurin-18-methyl Ester (**1**). Rhodobacter spheroids* in La Salle growth medium (350 mL, about 440 g) was dissolved in 800 mL of 1-propanol. It was filtered, and 20 g of KOH was added to the filtrate. The reaction mixture was stirred at room temperature for 1 h under a stream of air bubbled through the solution. It was then extracted with CH_2Cl_2/THF after adjusting the pH between 2.5 and 3. The organic layer was dried over sodium sulfate. Evaporation of the solvent gave a purple residue, which was dissolved in THF (150 mL) after which the solvent was evaporated. This process was repeated several times until there was no absorption at 756 nm and the appearance of a strong peak at 813 nm was evident. After evaporating the solvent, the crude 3-acetyl-purpurin-18 carboxylic acid thus obtained was converted into the corresponding methyl ester by treating with diazomethane. The residue was chromatographed on a silica column, eluting with acetone/CH_2Cl_2 (2% v/v), and the title compound was obtained as purple-red crystals after crystallizing from CH_2Cl_2/*n*-hexane. Yield: 650 mg. Mp: 272 °C. UV−vis in CH_2Cl_2 (λ_{max}, nm; ϵ_{max}, M^{-1} cm^{-1}): 364 (8.9×10^4), 412 (5.4×10^4), 545 (3.4×10^4), 777 (1.1×10^4), 815 (5.5×10^4). ^{1}H NMR (400 MHz, $CDCl_3$) δ (ppm): 9.21(s, 1H, 5-H), 8.78 (s, 1H, 10-H), 8.62 (s, 1H, 20-H), 5.13 (m, 1H, 17-H), 4.30 (m, 2H, 1H for 7-H, 1H for 18-H), 4.08 (m, 1H, 8-H), 3.63 (s, 3H, 12-CH_3), 3.57 (s, 3H, $-CO_2CH_3$), 3.52 (s, 3H, 2-CH_3), 3.15 (s, 3H, CH_3CO), 2.70 (m, 1H, $-CHHCH_2CO_2CH_3$), 2.42 (m, 2H, 8-CH_2CH_3), 2.35 (m, 1H, $-CHHCH_2CO_2CH_3$), 2.00 (m, 2H, $-CH_2CH_2CO_2CH_3$), 1.80 (d, $J = 7.2$ Hz, 3H, 7-CH_3), 1.70 (d, $J = 6.8$ Hz, 3H, 18-CH_3), 1.1 (t, $J = 6.5$ Hz, 3H, 8-CH_2CH_3), −0.30 (s, 1H, NH), −0.65 (s, 1H, NH). Anal. Calcd for $C_{34}H_{36}N_4O_5 \cdot H_2O$: C, 66.42; H, 6.24; N, 9.12. Found: C, 66.30; H, 5.90; N, 8.99. Mass Calcd for $C_{34}H_{36}N_4O_6$: 596.3. Found: *m*/*e* 596.8 (M + 1).

*3-Acetyl-bacteriopurpurin-18-N-hexylimide Methyl Ester (**3**).* 3-Acetyl-bacteriopurpurin-18 methyl ester **1** (180 mg) dissolved in CH_2Cl_2 (20 mL) was treated with a large excess of hexylamine (0.5 mL) at room temperature for 24 h. The disappearance of the 813 nm band and the appearance of a new 753 nm band indicated formation of the intermediate amide analogue. The solvent and the excess of amine were then evaporated under high vacuum (<30 °C) to give a residue, which was redissolved in CH_2Cl_2 and treated with diazomethane and to which a catalytic amount of methanolic KOH (3 to 4 drops) was added. The reaction mixture was stirred at room temperature for 1−2 min. The disappearance of the absorption band at 753 nm and the appearance of a new peak at 822 nm indicated completion of the reaction. After standard workup, the residue was chromatographed over a silica column, eluting with acetone/CH_2Cl_2 (2% v/v). The appropriate fractions were combined. The major band was collected, and the residue obtained after removing the solvent was crystallized from CH_2Cl_2/*n*-hexane as purple-red crystals. Yield: 120 mg (58%). Mp: 260 °C. UV−vis in CH_2Cl_2 (λ_{max}, nm; ϵ_{max}, M^{-1} cm^{-1}): 364 (6.1×10^4), 413 (3.6×10^4), 545 (2.6×10^4), 753 (5.7×10^3), 822 (4.9×10^4). ^{1}H NMR (400 MHz, $CDCl_3$) δ (ppm): 9.24 (s, 1H, 5-H), 8.80 (s, 1H, 10-H), 8.64 (s, 1H, 20-H), 5.33 (m, 1H, 17-H), 4.43 (t, $J = 6.03$ Hz, 2H, $-NCH_2(CH_2)_4CH_3$), 4.3 (m, 2H, 1H for 7-H, 1H for 18-H), 4.10 (m, 1H, 8-H), 3.71 (s, 3H, 12-CH_3), 3.58 (s, 3H, $-CO_2CH_3$), 3.54 (s, 3H, 2-CH_3), 3.16 (s, 3H, CH_3CO-), 2.68 (m, 1H, $-CHHCH_2CO_2CH_3$), 2.38 (m, 3H, 1H for $-CHHCH_2CO_2H_3$, 2H for 8-CH_2CH_3), 1.97 (m, 2H, $-NCH_2CH_2(CH_2)_3CH_3$), 1.82 (d, $J = 6.90$ Hz, 3H, 7-CH_3), 1.74 (d, $J = 6.9$ Hz, 3H, 18-CH_3), 1.60 (m, 2H, $-CH_2CH_2$-CO_2CH_3), 1.42 (m, 4H, $-NCH_2CH_2CH_2CH_2$ CH_2CH_3), 1.28

(m, 2H, $-(CH_2)_4CH_2CH_3$), 1.10 (t, $J = 6.9$ Hz, 3H, 8-CH_2CH_3), 0.95 (t, $J = 7.6$ Hz, 3H, $N(CH_2)_5CH_3$), −0.5 (s, 1H, NH), −0.72 (s, 1H, NH). MS Calcd for $C_{40}H_{49}N_5O_5$: 679.3. Found: *m/e* 680.5 (M + 1).

*3-Vinyl-bacteriopurpurin-18-N-hexylimide Methyl Ester (**2**).* Bacteriochlorin **3** (40 mg) was dissolved in dichloromethane (15 mL) and reacted with sodium borohydride (100 mg) at room temperature. The reaction was monitored by TLC. After completion of the reaction, it was diluted with dichloromethane (100 mL). The organic layer was washed with water (2 × 200 mL) and dried over sodium sulfate. Evaporation of the solvent afforded the corresponding 3-(1′-hydroxy)ethyl bacteriochlorin, which was isolated in quantitative yield (40 mg). It was redissolved in *o*-dichlorobenzene (5 mL), and the solution was maintained at 140−145 °C for 2 min. The reaction mixture was cooled to room temperature and chromatographed over a silica column, eluting first with hexane to remove the *o*-dichlorobenzene; further elution with acetone/CH_2Cl_2 (2% v/v) gave the title compound. Yield: 27 mg (70%). Mp: 245 °C. UV−vis in CH_2Cl_2 (λ_{max}, nm; ϵ_{max}, M^{-1} cm^{-1}): 366 (1.0×10^5), 417 (4.5×10^4), 538 (3.9×10^4), 740 (1.3×10^4), 796 (5.6×10^4). ^{1}H NMR (400 MHz, $CDCl_3$) δ (ppm): 8.58 (s, 1H, 5-H), 8.46 (s, 1H, 10-H), 8.35 (s, 1H, 20-H), 7.75 (dd, $J_1 = 11.9$ Hz, $J_2 = 18.3$ Hz, 1H, 3-C*H*═CH_2), 6.16 (d, $J = 18.3$ Hz, 1H, 3-CH═C*H*H), 6.05 (d, $J = 11.9$ Hz, 1H, 3-CH═CH*H*), 5.25 (m, 1H, 17-H), 4.41 (m, 2H, $-NCH_2(CH_2)_4CH_3$), 4.19 (m, 2H, 1H for 7-H, 1H for 18-H), 4.00 (m, 1H, 8-H), 3.62 (s, 3H, 12-CH_3), 3.55 (s, 3H, $-CO_2CH_3$), 3.26 (s, 3H, 2-CH_3), 2.63 (m, 1H, $-CHHCH_2CO_2CH_3$), 2.33 (m, 3H, 1H for-CH*H*$CH_2CO_2CH_3$, 2H for 8-CH_2CH_3), 1.95 (m, 2H, $-NCH_2CH_2(CH_2)_3CH_3$), 1.77 (d, $J = 7.1$ Hz, 3H, 7-CH_3), 1.69 (d, $J = 7.7$ Hz, 3H, 18-CH_3), 1.58 (m, 4H, 2H for $-N(CH_2)_2CH_2$ $(CH_2)_2CH_3$, 2H for CH_2CH_2-CO_2CH_3), 1.42 (m, 4H, $-N(CH_2)_3CH_2CH_2CH_3$), 1.09 (t, $J = 7.2$ Hz, 3H, 8-CH_2CH_3), 0.92 (t, $J = 6.9$ Hz, 3H, $-N(CH_2)_5CH_3$), −0.01 (s, 1H, NH), −0.354 (s, 1H, NH). MS Calcd for $C_{40}H_{49}N_5O_4$: 663.4. Found: *m/e* 663.5.

*3-Formyl-bacteriopurpurin-18-N-hexylimide Methyl Ester (**4**).* The vinyl derivative **2** (100 mg) was dissolved in THF (30 mL) after which osmium tetroxide (30 mg) in ether (3 mL) and sodium periodate (200 mg) in water (10 mL) were added. The reaction mixture was then left stirring at room temperature for 20 h under a nitrogen atmosphere. The completion of the reaction was monitored by UV−vis spectrophotometry. The disappearance of the long-wavelength absorption band at 796 nm and the appearance of a new band at 830 nm indicated completion of the reaction. The reaction mixture was then extracted with dichloromethane, washed with 2% acetic acid/water solution, and washed again with water (3 × 200 mL). After standard workup, the residue was purified by preparative chromatography, and the title compound was obtained. Yield 50 mg (50%). Mp: 265 °C. UV−vis in CH_2Cl_2 (λ_{max}, nm; ϵ_{max}, M^{-1} cm^{-1}): 364 (8.0×10^4), 412 (4.3×10^4), 548 (3.6×10^4), 795 (1.5×10^4), 829 (8.2×10^4). ^{1}H NMR (400 MHz, $CDCl_3$) δ (ppm): 11.28 (s, 1H, −CHO), 9.38 (s, 1H, 5-H), 8.80 (s, 1H, 10-H), 8.63 (s, 1H, 20-H), 5.30 (m, 1H, 17-H), 5.00 (m, 2H, $-NCH_2(CH_2)_4CH_3$), 4.42 (m, 2H, 1H for 7-H, 1H for 18-H), 4.12 (m, 1H, 8-H), 3.71 (s, 3H, 12-CH_3), 3.62 (s, 3H, CO_2-CH_3), 3.57 (s, 3H, 2-CH_3), 2.67 (m, 1H, C*H*H$CH_2CO_2CH_3$), 2.36 (m, 3H, 1H for CH*H*$CH_2CO_2CH_3$, 2H for 8-CH_2CH_3), 1.96 (m, 2H, $NCH_2CH_2(CH_2)_3CH_3$), 1.84 (d, $J = 7.1$ Hz, 3H, 7-CH_3), 1.73 (d, $J = 7.6$ Hz, 3H, 18-CH_3), 1.57 (m, 2H, $CH_2CH_2CO_2$-CH_3), 1.43 (m, 4H, $N(CH_2)_2CH_2CH_2CH_2CH_3$), 1.26 (m, 2H, $N(CH_2)_4CH_2CH_3$), 1.11 (t, $J = 7.2$ Hz, 3H, 8-CH_2CH_3), 0.94 (t, $J = 7.0$ Hz, 3H, $N(CH_2)_5CH_3$), −0.51 (s, 1H, NH), −0.65 (s, 1H, NH). MS Calcd for $C_{39}H_{47}N_5O_5$: 665.4. Found: *m/e* 666.3 (M + 1).

*3-(1-Nonyloxy) Ethyl-purpurin-18-N-hexylimide Methyl Ester (**5**).* The 3-(1-hydroxy) ethyl bacteriochlorin (40 mg) was dissolved in dry dichloromethane (5.0 mL), after which HBr gas was bubbled through the solution for 2 min and the solution was stirred at room temperature under an argon atmosphere for 5 min. The solvent and excess of hydrogen bromide were then evaporated under high vacuum (<30 °C) to give a residue, which was not characterized but immediately redissolved in dry dichloromethane (5.0 mL) and reacted with 1-nonanol (1.0 mL) in the presence of anhydrous potassium carbonate (200 mg). The reaction mixture was stirred for 30 min. After standard workup, the residual 1-nonanol was removed under high vacuum. The crude product was chromatographed on a silica column, eluting with acetone/CH_2Cl_2 (2% v/v), and the title compound was obtained. Yield: 41 mg (86.5%). UV−vis in CH_2Cl_2 (λ_{max}, nm; ϵ_{max}, M^{-1} cm^{-1}): 367 (1.1×10^5), 417 (5.8×10^4), 536 (4.0×10^4), 750 (1.4×10^4), 787 (4.8×10^4). ^{1}H NMR (400 MHz, $CDCl_3$) δ (ppm): 8.86 (s, 0.5H, $^1/_2 \times$ 5-H), 8.82 (s, 0.5H, $^1/_2 \times$ 5-H), 8.62 (s, 1H, 10-H), 8.33 (s, 1H, 20-H), 5.66 (m, 1H, 3-$CH_3CH(O(CH_2)_8CH_3)-$), 5.28 (m, 1H, 17-H), 4.43 (m, 2H, $-NCH_2(CH_2)_4CH_3$), 4.20 (m, 2H, 1H for 4-H, 1H for 18-H), 4.03 (m, 1H, 8-H), 3.62 (s, 3H, 12-CH_3), 3.59 (m, 2H, $-CH_2(CH_2)_7CH_3$), 3.56 (s, 3H, $-CO_2CH_3$), 3.22 (s, 1.5H, $^1/_2 \times$ 2-CH_3), 3.21 (s, 1.5H, $^1/_2 \times$ 2-CH_3), 2.63 (m, 1H, $-CHHCH_2CO_2CH_3$), 2.32 (m, 3H, 1H for $-CH_2CHHCO_2CH_3$, 2H for 8-CH_2CH_3), 1.99 (d, $J = 6.6$ Hz, 3H, 3-$CH_3CH(OC_9H_{19})$, 1.98 (m, 2H, $-NCH_2CH_2(CH_2)_3CH_3$), 1.79 (2d, $J = 7.2$ Hz, overlapped, 3H, 7-CH_3), 1.69 (d, $J = 7.0$ Hz, 4H, 1H for $-CH_2CHHCO_2CH_3$, 3H for 18-CH_3), 1.60 (m, 3H, 1H for $-CH_2CHHCO_2CH_3$, 2H for $-CH_2CH_2(CH_2)_6CH_3$), 1.44 (m, 4H, $NCH_2CH_2CH_2CH_2CH_2CH_3$), 1.36−1.08 (m, 17H, 2H for $-N(CH_2)_4CH_2CH_3$, 3H for 8-CH_2CH_3, 12H for $-OCH_2CH_2$-$(CH_2)_6CH_3$), 0.93 (t, 3H, $J = 6.8$ Hz, $-N(CH_2)_5CH_3$), 0.78 (m, 3H, $-O(CH_2)_8$ CH_3), 0.10 (s, 1H, NH), −0.30 (s, 1H, NH). MS Calcd for $C_{49}H_{69}N_5O_5$: 807.5. Found: *m/e* 808.9 (M + 1).

Photophysical Measurements. Absorption spectra were recorded on a Hewlett-Packard 8453A diode array spectrophotometer. Time-resolved fluorescence and phosphorescence spectra were measured by a Photon Technology International GL-3300 with a Photon Technology International GL-302 nitrogen laser/pumped dye laser system equipped with a four-channel digital delay/pulse generator (Stanford Research System Inc. DG535) and a motor driver (Photon Technology International MD-5020). Excitation wavelengths were from 538 to 551 nm using coumarin 540A (Photon Technology International, Canada) as a dye. Fluorescence lifetimes were determined by a single exponential curve fit using a microcomputer. Nanosecond transient absorption measurements were carried out using a Nd:YAG laser (Continuum, SLII-10, 4−6 ns fwhm) at 355 nm with the power of 10 mJ as an excitation source. Photoinduced events were estimated by using a continuous Xe lamp (150 W) and an InGaAs-PIN photodiode (Hamamatsu 2949) as a probe light and a detector, respectively. The output from the photodiodes and a photomultiplier tube was recorded with a digitizing oscilloscope (Tektronix, TDS3032, 300 MHz). The transient spectra were recorded using fresh solutions in each laser excitation. All experiments were performed at 298 K.

For the $^1O_2$ phosphorescence measurements, an O_2-saturated C_6D_6 solution containing the sample in a quartz cell (optical path length 10 mm) was excited at $\lambda = 532$ nm using a Cosmo System LVU-200S spectrometer. A photomultiplier (Hamamatsu

CHART 1

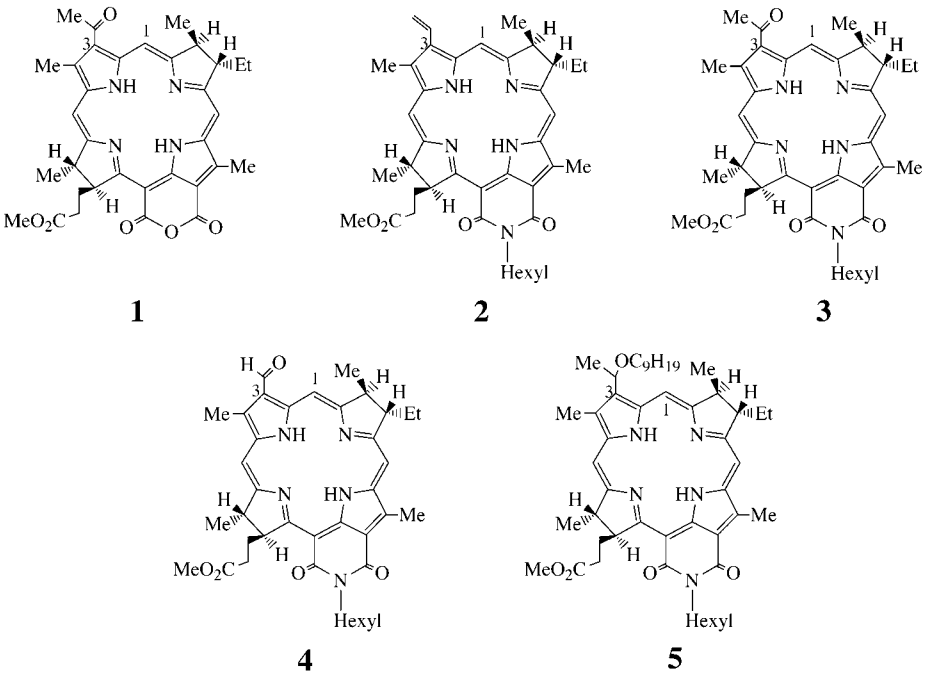

Photonics, R5509-72) was used to detect emission in the near-infrared region (band path 1 mm).

Electrochemical and Spectroelectrochemical Measurements. Cyclic voltammetry (CV) measurements were performed at 298 K on an EG&G model 173 potentiostat coupled with an EG&G model 175 universal programmer in deaerated benzonitrile solution containing 0.10 M TBAP as a supporting electrolyte. A three-electrode system was utilized and consisted of a glassy carbon working electrode, a platinum wire counter electrode, and a saturated calomel reference electrode (SCE). The reference electrode was separated from the bulk of the solution by a fritted-glass bridge filled with the solvent/supporting electrolyte mixture. Thin-layer spectroelectrochemical measurements of the one-electron oxidized and one-electron reduced bacteriochlorin derivatives were carried out using an optically transparent platinum thin-layer working electrode and a Hewlett-Packard model 8453 diode array spectrophotometer coupled with an EG&G model 173 universal programmer.

ESR Measurements. ESR measurements were performed in benzonitrile (PhCN) with a JEOL X-band spectrometer (JES-RE1XE). The ESR spectra were recorded under nonsaturating microwave power conditions. The magnitude of modulation was chosen to optimize the resolution and the signal-to-noise (S/N) ratio of the observed spectra. The *g* values were calibrated with a Mn^{2+} marker. Computer simulation of the ESR spectra was carried out by using Calleo ESR version 1.2 (Calleo Scientific Publisher) on a Macintosh personal computer.

Theoretical Calculations. Density functional theory (DFT) calculations were performed on a COMPAQ DS20E computer. Geometry optimizations were carried out using the B3LYP functional and 6-31G basis set[26,27] with the unrestricted Hartree−Fock (UHF) formalism and the BLYP functional and 3-21G basis set[26,27] with the restricted Hartree−Fock (RHF) formalism as implemented in the Gaussian 98 program.[28]

Results and Discussion

Photophysical Properties. The investigated compounds are shown in Chart 1. Compounds **1**−**5** exhibit long-wavelength absorption (788−831 nm) as compared to the corresponding chlorin derivatives, which have absorptions at shorter than 700 nm. A typical absorption spectrum is shown in Figure 1 for bacteriochlorin **4**, which has the Q_y band ($a_{1u} \rightarrow e_{gx}$ transition) at 831 nm, the Q_x band ($a_{2u} \rightarrow e_{gy}$ transition) at 551 nm, and the split Soret band at 367 and 416 nm in PhCN. Such a long-wavelength Q_y band is highly promising for the compound's potential use in photodynamic therapy. The absorption maxima of **1**−**5** are listed in Table 1. The Q_y bands of the compounds are located between 788 and 831 nm and are significantly red-shifted as compared to the Q_y band of bacteriochlorophyll *a* (BChla) (771 nm), whereas the Q_x bands of **1**−**5** (538−551 nm) are blue-shifted compared to the Q_x band of BChla which is located at 594 nm.[18] The imide ring system (**3**) exhibits a longer-wavelength absorption (824 nm) as compared to the corresponding anhydride system (**1**) (815 nm). The difference between **3** and **4** is the substituent at position-3 (acetyl vs formyl), and the formyl compound **4** has the longest-wavelength absorption (831 nm) among the investigated compounds. When the vinyl group in **2** at position 3 is replaced by an alkyl ether side chain in **5**, the Q_y band is blue-shifted from 799 to 788 nm.

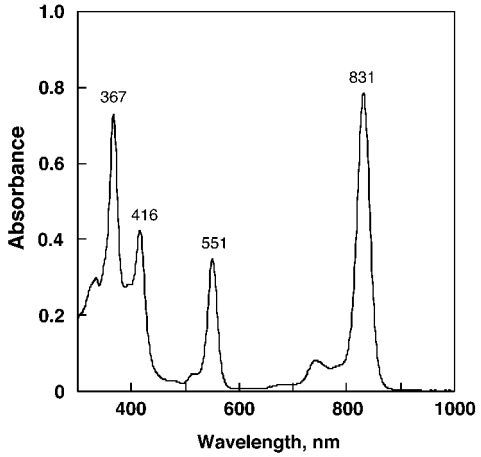

Figure 1. UV−vis absorption spectrum of **4** (1.3×10^{-5} M) in PhCN at 298 K.

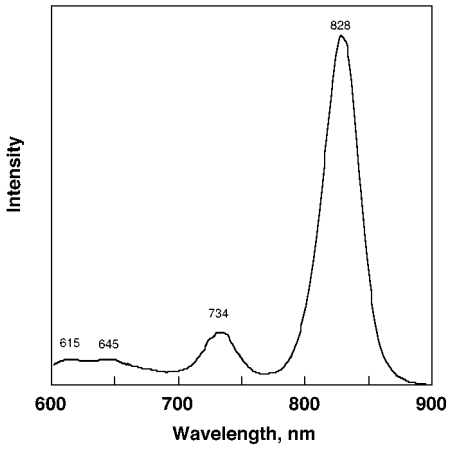

Figure 2. Fluorescence spectrum of **1** (8.0×10^{-6} M) in deaerated PhCN at 3 ns after laser excitation (548 nm) at 298 K.

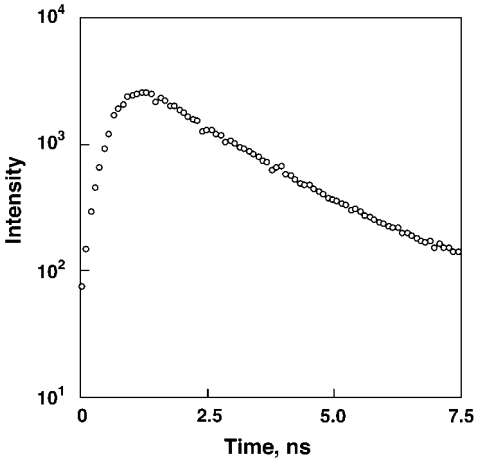

Figure 3. Fluorescence decay of **1** (4.0×10^{-6} M) in deaerated PhCN at 298 K by excitation (548 nm) at $\lambda_{em} = 828$ nm.

A typical fluorescence spectrum of the compounds is shown in Figure 2 for the case of **1**. The Stokes shift is rather small because the fluorescence maximum at 828 nm is only slightly red-sifted as compared to the absorption maximum at 815 nm.

The fluorescence decay of **1** is fitted well by a single-exponential line with lifetimes of 1.3 ns as shown in Figure 3.[29] The data for this compound and the other bacteriochlorin derivatives are summarized in Table 1. The singlet-excited-state energies [*E*(S)] determined from the absorption and fluorescence maxima are also listed in Table 1. The *E*(S) energies lie between 1.48 and 1.56 eV (Table 1) and are the lowest ever reported among this class of compounds.[1−4]

The short fluorescence lifetimes of **1**−**5** may be ascribed to the fast intersystem crossing to generate a triplet excited state.

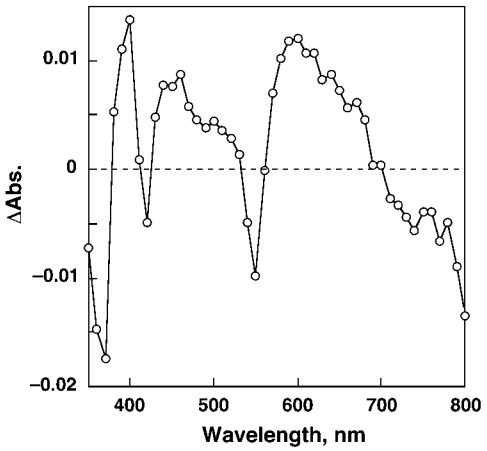

Figure 4. T−T absorption spectrum of **1** (8.0×10^{-6} M) obtained by the laser flash photolysis in deaerated PhCN at 2.0 μs after laser excitation (355 nm) at 298 K.

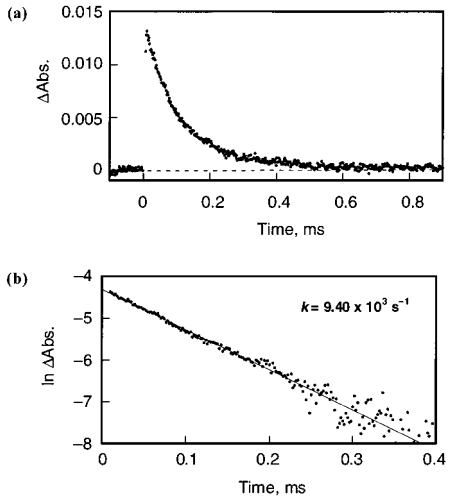

Figure 5. Kinetic trace (a) and first-order plot (b) for the T−T absorption of **1** (8.0×10^{-6} M) at 400 nm in deaerated PhCN.

In fact, phosphorescence spectra are observed in deaerated frozen 2-MeTHF at 77 K. The phosphorescence maxima and the triplet excited-state energies are summarized in Table 1.

The triplet excited states of **1**−**5** are also detected from the transient absorption spectra measured 2.0 μs after laser excitation at 355 nm. A typical example is shown in Figure 4 for the case of **1**. The negative absorptions at 370, 420, 550, and 800 nm in Figure 4 are due to bleaching of the ground-state absorption bands seen in Figure 1. The positive absorptions at 400, 460, and 600 nm in Figure 4 are due to the triplet−triplet (T−T) transition. The T−T absorption decay obeys first-order kinetics as shown in Figure 5. This indicates that there is no contribution

TABLE 1: Photophysical Data of Bacteriochlorins in PhCN

	abs, λ_{max}, nm	fluorescence,	singlet excited state		phosphorescence		triplet excited state	
compd	(10^{-4} ϵ_{max}, M^{-1} cm^{-1})	λ_{max}, nm	τ, ns	*E*(S), eV	λ_{max}, nm	*E*(T), eV	λ_{max}(T−T), nm	τ(T−T), s
1	366 (4.10), 415 (2.63), 548 (1.68), 815 (2.63)	734, 828	1.3	1.51	854	1.45	400, 460, 600	1.1×10^{-4}
2	370 (8.15), 421 (3.90), 543 (3.28), 799 (4.31)	714, 817	1.4	1.53	845	1.47	400, 450, 580	1.1×10^{-4}
3	367 (5.97), 417 (3.17), 548 (2.47), 824 (5.16)	740, 835	1.2	1.50	870	1.42	400, 440, 600	8.6×10^{-5}
4	367 (5.95), 416 (3.47), 551 (2.87), 831 (6.38)	742, 842	1.1	1.48	860	1.44	400, 440, 640	7.2×10^{-5}
5	369 (11.83), 419 (6.23), 538 (4.71), 788 (5.69)	706, 804	1.4	1.56	840	1.48	400, 460, 570	1.5×10^{-4}

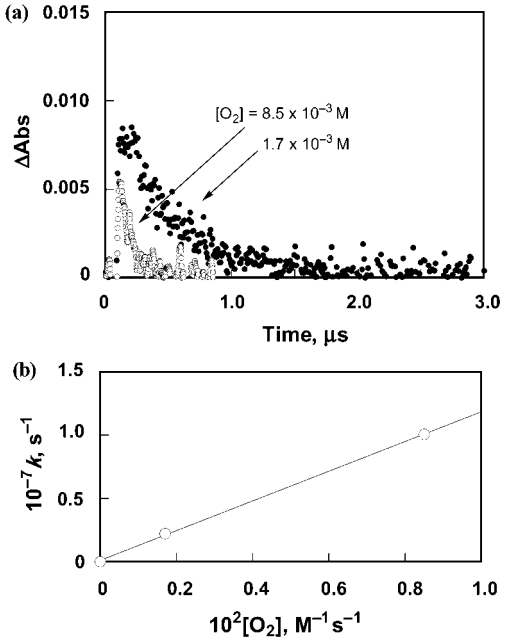

Figure 6. Kinetic trace (a) for the T−T absorption of **1** (8.0×10^{-6} M) at 400 nm in air- and O_2-saturated PhCN at 298 K and (b) plot of decay rate constant (k) vs [O_2].

TABLE 2: Quenching Rate Constants ($k_q(O_2)$) of Triplet Excited States of Bacteriochlorins by O_2 in PhCN and Relative Quantum Yields ($\Phi(^1O_2)$) of Singlet Oxygen Generated by Irradiation of Bacteriochlorins in Oxygen-Saturated C_6D_6 at 298 K

compound	$k_q(O_2)$, M^{-1} s^{-1}	$\Phi(^1O_2)$[a]
1	1.2×10^9	0.48
2	1.7×10^9	0.55
3	1.1×10^9	0.33
4	1.5×10^9	0.41
5	1.5×10^9	0.45
C_{60}[b]	2.0×10^9 [c]	0.96

[a] Excitation at $\lambda = 532$ nm, using C_{60} ($\Phi(^1O_2) = 0.96$ in C_6D_6) as standard. [b] Taken from ref 31. [c] In C_6H_6.

of the triplet−triplet annihilation under the present experimental conditions. The T−T absorption maxima and the triplet lifetimes are summarized in Table 1. The triplet lifetimes are in the range of 72−150 μs.

The decay of the T−T absorption in oxygen-saturated PhCN is enhanced significantly over what is observed in deaerated PhCN. This is shown in Figure 6 for compound **1**. The decay kinetics obey first-order kinetics, and the decay rate constant increases with increasing oxygen concentration. Thus, an efficient energy transfer from the triplet excited state of **1** to oxygen occurs to produce singlet oxygen. The rate constant of the energy transfer was determined as 2×10^9 M^{-1} s^{-1} from the dependence of the decay rate constant on oxygen concentration. This value is close to the diffusion-limited value in PhCN (3.4×10^9 M^{-1} s^{-1}).[12,30]

Irradiation of an oxygen-saturated benzene solution of **1** results in formation of singlet oxygen, which was detected by the $^1O_2$ phosphorescence at 1270 nm (see Experimental Section). Quantum yields (Φ) of $^1O_2$ generation were determined from the phosphorescence intensity, which was compared to the intensity obtained using a C_{60} reference compound.[31] Relatively high Φ values are obtained and are summarized in Table 2 in which the highest Φ value is 0.55 for **2**.

Redox Processes. Figure 7 shows cyclic voltammograms of **1**−**5**, arranged according to the ease of oxidation. Compound **5**

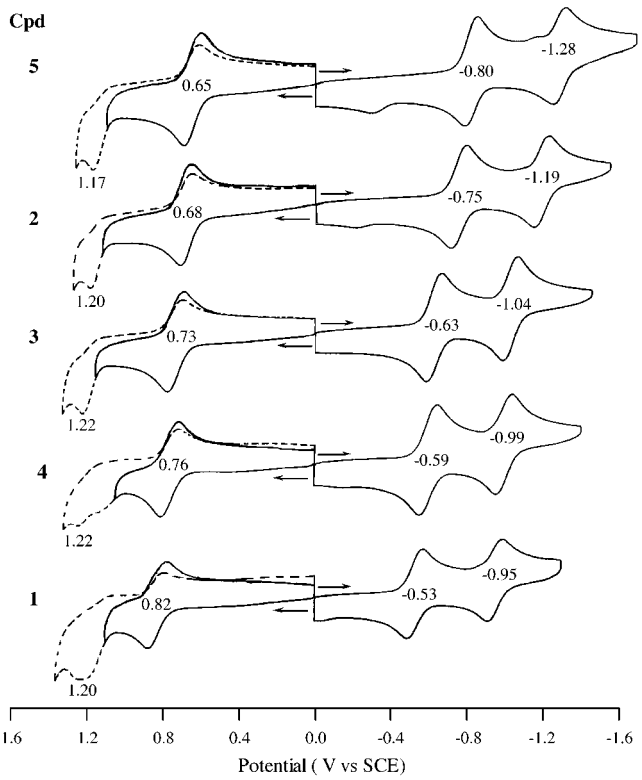

Figure 7. Cyclic voltammograms of **1**−**5** in PhCN containing 0.1 M TBAP.

is the easiest to oxidize and the hardest to reduce among the investigated compounds. The first and second ring oxidations of **5** occur at $E_{1/2} = 0.65$ V and $E_p = 1.17$ V, whereas the first and second reversible ring reductions occur at $E_{1/2} = -0.80$ V and −1.28 V. The difference between redox potentials for formation of the monocation and the dication ($E_{ox2} - E^0_{ox1} = 0.52$ V) and the difference between those for formation of the monoanion and the dianion ($E^0_{red1} - E^0_{red2} = 0.48$ V) are in the same range as those reported for related porphyrins.[32,33] In contrast, the difference between the reversible half-wave potentials for formation of the monocation and monoanion ($|E^0_{ox1} - E^0_{red1}| = 1.45$ V), which corresponds to the HOMO (highest occupied molecular orbital)−LUMO (lowest unoccupied molecular orbital) gap, is significantly smaller than the difference generally observed for porphyrins (2.1−2.4 V) having planar macrocycles such as TPP (TPP^{2-} = the dianion of tetraphenylporphyrin) or OEP (OEP^{2-} = the dianion of octaethylporphyrin). The experimentally observed HOMO−LUMO gap of **1**−**5** is also smaller than the gap of 1.9−2.1 V often seen for a number of nonplanar porphyrins.[33] Similar redox processes are observed for all five bacteriochlorin derivatives (Figure 7), and the redox potentials for these compounds are listed in Table 3.

The much smaller values of $|E^0_{ox1} - E^0_{red1}|$ in Table 3 as compared to those of nonplanar porphyrins is ascribed to a decrease in the HOMO level of compounds **1**−**5** with increasing peripheral saturation.[5] The $|E^0_{ox1} - E^0_{red1}|$ values (1.35−1.45 V) for **1**−**5** are even smaller than the experimental value reported for BChla (1.59 V),[18] which agrees with the calculated value of the HOMO−LUMO gap of BChla (1.54 eV).[34] The $|E^0_{ox1} - E^0_{red1}|$ values of **1**, **3**, and **4** (1.35−1.36 eV), which have long-wavelength Q_y bands at 815, 824, and 831 nm, are smaller than the $|E^0_{ox1} - E^0_{red1}|$ of **2** and **5**, which have Q_y bands at 799 and 788 nm, respectively. Because the E^0_{ox1} values in Table 3

TABLE 3: Half-wave Potentials (V vs SCE) of Bacteriochlorins in PhCN Containing 0.1 M TBAP

	oxidation			reduction			
compd	second	first	$E_{ox2} - E^0_{ox1}$	first	second	$E^0_{red1} - E^0_{red2}$	$E^0_{ox1} - E^0_{red1}$
1	1.20[a]	0.82	0.38	−0.53	−0.95	0.42	1.35
2	1.20[a]	0.68	0.52	−0.75	−1.19	0.44	1.43
3	1.22[a]	0.73	0.49	−0.63	−1.04	0.41	1.36
4	1.22[a]	0.76	0.46	−0.59	−0.99	0.40	1.35
5	1.17[a]	0.65	0.52	−0.80	−1.28	0.48	1.45

[a] The peak potential E_p is taken as E_{ox2}, scan rate at 100 mV/s.

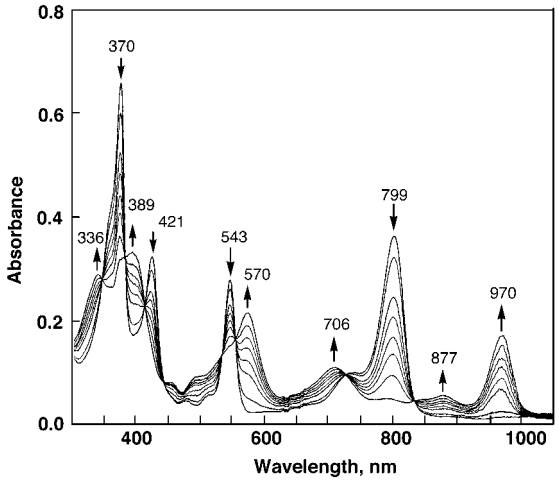

Figure 8. The UV−visible spectral changes of **2** upon the first reduction at −0.90 V in PhCN contanining 0.2 M TBAP.

(0.65−0.82 V) are more positive than the E^0_{ox1} value of BChla (0.35 V),[18] the decrease in $|E^0_{ox1} - E^0_{red1}|$ as compared to that of BChla results from less negative values of E^0_{red1}. This means that the bacteriochlorin derivatives examined in this study have higher HOMO levels but much lower LUMO levels than in the case of BChla.

The HOMO−LUMO gap of **1** was calculated using the density functional theory (DFT) with the BLYP functional and 3-21G basis set (see Experimental Section).[26,27] The calculated value (1.25 eV) agrees with the $|E^0_{ox1} - E^0_{red1}|$ value (1.35 V). The calculated HOMO−LUMO gap becomes larger with increasing degree of macrocycle conjugation, that is, 1.25 eV for the bacteriochlorin **1**, 1.41 eV for the corresponding chlorin and 1.45 V for the corresponding porphyrin.[5,35]

Radical Anions and Cations. The UV−visible spectra obtained during the first reduction step of **2** shows clear isosbestic points as seen in Figure 8. The formation of a π radical anion of **2** results in a disappearance of the Q_y band at 799 nm and the appearance of new absorption bands at longer wavelengths (877 and 970 nm) as has also been reported upon oxidation of BChla.[17,18] Reoxidation of the monoanion of **2** to the neutral species is reversible, and the spectrum is regenerated without loss of spectral intensity. The NIR band at 970 nm in the case of $\mathbf{2}^{\bullet-}$ and 948−990 nm for the other electrogenerated monoanions can be designated as a marker band of the π radical anions of bacteriochlorins.[21]

The UV−visible absorption spectra obtained during the first one-electron oxidation of **2** show five clear isosbestic points as shown in Figure 9. This indicates that the electrogenerated radical cation is stable on the time scale of the measurement and does not undergo a chemical reaction on the time scale of the measurement.[36] The rereduction of the π radical cation to the neutral species is also reversible on the spectroelectrochemical time scale, and this result contrasts with the case of BChla in which a dehydrogenation product of BChla is clearly seen during the oxidation.[18] The disappearance of the Q_y band at 799 nm in the case of **2** is accompanied by the appearance of a new absorption band at 873 nm. The latter band is well-defined and can be used as a marker band of the bacteriochlorin radical cation. Marker bands are seen for the radical cations and radical anions of other investigated bacteriochlorins, and these values are listed in Table 4 with the other spectral data.

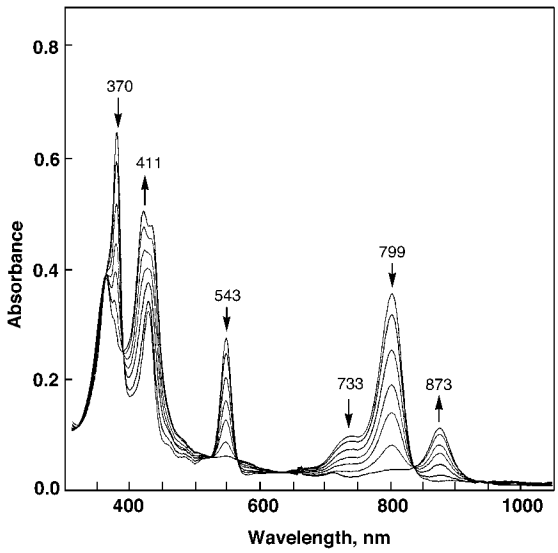

Figure 9. The UV−visible spectral changes of **2** upon the first oxidation at +1.00 V in PhCN containing 0.2 M TBAP.

TABLE 4: Spectroscopic Data of Radical Anions and Cations of Bacteriochlorins in PhCN Contaniing 0.2 M TBAP

compound	radical anion λ_{max}, nm ($10^{-4}\,\epsilon_{max}$, $M^{-1}\,cm^{-1}$)	radical cation λ_{max}, nm ($10^{-4}\,\epsilon_{max}$, $M^{-1}\,cm^{-1}$)
1	338 (1.49), 367 (2.08), 592 (1.16), 725 (0.57), 892 (0.22) 982 (0.90)	355 (2.49), 409 (3.28), 891 (0.51)
2	336 (3.45), 389 (3.98), 570 (2.49), 706 (1.10), 877 (0.60), 970 (2.02)	353 (5.20), 411 (5.83), 873 (1.45)
3	339 (2.25), 400 (2.79), 608 (1.60), 737 (0.64), 980 (0.16)	356 (3.82), 412 (4.17), 885 (0.30)
4	338 (2.37), 399 (3.06), 628 (1.60), 739 (0.78), 912 (0.36), 990 (0.79)	364 (3.37), 414 (3.82), 896 (0.25)
5	327 (4.68), 372 (6.83), 547 (2.87), 690 (1.58), 865 (0.65), 948 (2.24)	352 (6.24), 419 (10.11), 866 (1.11)

The one-electron oxidized product, $\mathbf{3}^{\bullet+}$, and one-electron reduced product, $\mathbf{3}^{\bullet-}$, were also characterized by ESR spectroscopy. Singly oxidized **3** was generated by chemical oxidation of the neutral compound with 1 equiv of $Ru(bpy)_3(PF_6)_3$ (E^0_{red} = 1.24 V vs SCE)[37] in PhCN at 298 K. The ESR spectrum of $\mathbf{3}^{\bullet+}$ thus obtained is shown in Figure 10a. The g value is determined as $g = 2.0037$ and is slightly larger than the reported g value of the radical cation of $[(TPC)Zn]^{\bullet+}$ (TPC^{2-} = the dianion of tetraphenylchlorin), $g = 2.0030$.[38] ESR signals were also obtained for the radical cations of other investigated bacteriochlorins with g values of 2.0038 ($\mathbf{1}^{\bullet+}$), 2.0034 ($\mathbf{2}^{\bullet+}$), 2.0030 ($\mathbf{4}^{\bullet+}$), and 2.0035 ($\mathbf{5}^{\bullet+}$). However, the hyperfine structures were not sufficiently resolved to determine the hyperfine coupling constants except for $\mathbf{3}^{\bullet+}$. The hyperfine splitting due to nitrogens and protons of $\mathbf{3}^{\bullet+}$ is well-resolved, and the

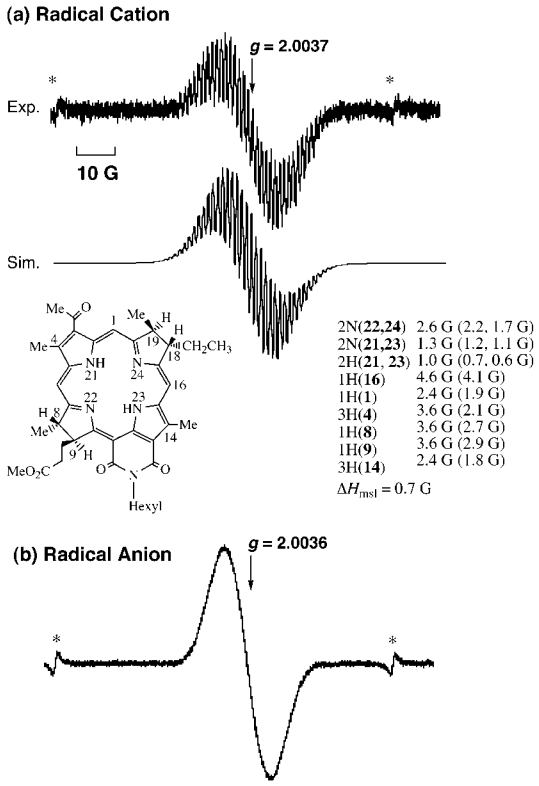

Figure 10. ESR spectrum of radical cation of **3** (a) generated in the reaction of **3** (1.0×10^{-3} M) with $Ru(bpy)_3(PF_6)_3$ (1.0×10^{-3} M) and hyperfine coupling contants with maximum slope line widths (ΔH_{msl}). The values in parentheses are those determined by DFT calculation. Panel b shows the ESR spectrum of radical anion of **3** genarated in the reaction of **3** (1.0×10^{-3} M) with naphthalene radical anion (1.0×10^{-3} M). Asterisk denotes Mn^{2+} marker.

hyperfine coupling constants (hfc) are listed in Figure 10a where the computer simulation spectrum is shown for comparison. Assignment of the hfc values was made by comparison of the experimental data with the hfc values predicted by the DFT calculation (see Experimental Section). The calculated hfc values largely agree with the experimental values, demonstrating unsymmetric spin distribution due to the substituents on the macrocyclic ring. The hfc values of two nitrogens [2.6 G for N(22,24)] are significantly larger than the values of the other two nitrogens [1.3 G for N(21,23)]. The hfc values of nitrogens in $\mathbf{3}^{\bullet+}$ (2.6 and 1.3 G) are larger than the reported values of tetraphenylbacteriochlorin radical cation (1.20 and 1.19 G),[21b] in which the four nitrogens are nearly equivalent. On the other hand, there is no hyperfine splitting due to the protons at positions 18 and 19, and the hfc values of the protons at positions 8 and 9 (3.6 G) are much smaller than the reported value (8.0 G) of the eight equivalent protons at positions 8, 9, 18, and 19 of $[(TPB)Zn]^{\bullet+}$ (TPB^{2-} = the dianion of tetraphenylbacteriochlorin).[21b] Thus, the spin distribution in the radical cation of substituted bacteriochlorin, which has no symmetry (C_1), is altered significantly as compared to tetraphenylbacteriochlorin radical cation, which has D_{2h} symmetry.

The one-electron reduced product $\mathbf{3}^{\bullet-}$ was generated by chemical reduction of the neutral compound with 1 equiv of naphthalene radical anion ($E^0_{ox} = -2.29$ V vs SCE).[39] The resulting ESR spectrum of $\mathbf{3}^{\bullet-}$ is shown in Figure 10b. The g value of $\mathbf{3}^{\bullet-}$ (2.0036) (Figure 10b) is nearly the same as the value of $\mathbf{3}^{\bullet+}$ (2.0037) (Figure 10a). Unfortunately, the hyperfine splitting is not resolved in the case of $\mathbf{3}^{\bullet-}$ (Figure 10b), precluding determination of the hfc values.

Conclusions

In this paper, the first detailed photophysical and electrochemical investigation of substituted bacteriochlorin (**1**−**5**) is described. The Q_y bands of the compounds are significantly red-shifted as compared to the Q_y band of BChla; **4** has a Q_y band in the NIR region (831 nm), which is the longest ever reported among this class of compounds. Such a large red shift in the Q_y band is reflected in the one-electron redox potentials of the substituted bacteriochlorins; **4** has the smallest HOMO−LUMO gap as indicated by the smallest difference between the half-wave potentials, $|E^0_{ox1} - E^0_{red1}| = 1.35$ V. The marker bands of both the radical anion and radical cation are determined from the spectroelectrochemical data. The unsymmetrical spin distribution of the radical cation of bacteriochlorins was also determined for the first time by the ESR spectrum.

Acknowledgment. This work was supported by a Grant-in-Aid for Scientific Research Priority Area (Grant No. 11228205) from the Ministry of Education, Science, Culture, Sports, Science and Technology, Japan, the Robert A. Welch Foundation (K.M.K., Grant E-680), NIH (Grant CA 55791), and the shared resources of the Roswell Park Cancer Center Support Grant (P30CA16056). Mass spectrometry analyses were performed at the Mass Spectrometry Facility, Michigan State University, East Lansing, Michigan.

References and Notes

(1) (a) Pandey, R. K.; Zheng, G. *Pophyrins as Photosensitizers in Photodynamic Therapy*, In *The Porphyrin Handbook*, Kadish, K. M., Smith, K. M., Guilard, R., Eds.; Academic Press: San Diego, 2000; Vol. 6, Chapter 43. (b) Bonnett, R. *Chem. Soc. Rev*. **1995**, *24*, 19. (c) Pandey R. K.; Herman, C. *Chem. Ind. (London)* **1998**, 739.

(2) (a) Davis, S.; Weiss, M.; Wong, J. R.; Lampids, T. J.; Chen, L. B. *J. Biol. Chem.* **1985**, *260*, 13844. (b) Dolphin, D. *Can. J. Chem.* **1994**, *72*, 1005. (c) Li, G.; Chen, Y.; Missert, J. R.; Rungra, A.; Dougherty, T. J.; Grossman, Z. D.; Pandey, P. K. *J. Chem. Soc., Perkin Trans. 1* **1999**, 1785.

(3) Scheer, H.; Inhoffen, H. H. In *The Porphyrins*; Dolphin, D., Ed.; Academic Press: New York, 1978; Vol II, pp 45−90.

(4) Hanson, L. S. In *Chlorophylls*; Scheer, H., Ed.; CRC Press: Boca Raton, FL, 1991; pp 993−1014. (b) Plato, M.; Möbius, K.; Lubitz, W. In *Chlorophylls*; Scheer, H., Ed.; CRC Press: Boca Raton, FL, 1991; pp 1015−1046.

(5) Ghosh, A. *J. Phys. Chem. B* **1997**, *101*, 3290.

(6) (a) Stolzenberg, A. M.; Strauss, S. H.; Holm, R. H. *J. Am. Chem. Soc.* **1981**, *103*, 4763. (b) Stolzenberg, A. M.; Schussel, L. J. *Inorg. Chem.* **1991**, *30*, 3205.

(7) Hasegawa, J.; Ozeki, Y.; Ohkawa, K.; Hada, M.; Nakatsuji, H. *J. Phys. Chem. B* **1998**, *102*, 1320.

(8) Kessel, D.; Smith, K. M.; Pandey, R. K.; Shiau, F.-Y.; Henderson, B. *Photochem. Photobiol.* **1993**, *58*, 200.

(9) (a) Zheng, G.; Alderfer, J. L.; Senge, M. O.; Shibata, M.; Dougherty, T. J.; Pandey, R. K. *J. Org. Chem.* **1998**, *63*, 6434. (b) Jaquinod, J.; Senge, M. O.; Pandey, R. K.; Forsyth, T. P.; Smith, K. M. *Angew. Chem., Int. Ed. Engl.* **1996**, *35*, 1840. (c) Zheng, G.; Pandey, R. K.; Forsyth, T. P.; Kozyrev, A. N.; Dougherty, T. J.; Smith, K. M. *Tetrahedron Lett.* **1997**, *38*, 2409.

(10) (a) Mathis, P.; Rutherford, A. W. In *Photosyntheses*; Amesz, J., Ed.; Elsevier: Amsterdam, 1987; p 63. (b) *Anoxygenic Photosynthetic Bacteria*; Blankenship, R. E., Madigan, M. T., Bauer, C. E., Eds.; Kluwer Academic Publishers: Dordrecht, The Netherlands, 1995; pp 137−149.

(11) Michel-Beyerle, M. E.; Plato, M.; Deisenhoer, J.; Michel, H.; Bixon, M.; Jortner, J. *Biochim. Biophys. Acta* **1988**, *932*, 52.

(12) (a) Pandey, R. K.; Sumlin, A. B.; Potter, W. R.; Bellnier, B. W.; Henderson, S.; Constantine, S.; Aoudia, M.; Rodgers, M. R.; Smith, K. M.; Dougherty, T. J. *Photochem. Photobiol.* **1996**, *63*, 194. (b) Pandey, R. K.; Tsuchida, T.; Constantine, S.; Zheng, G.; Medforth, C.; Kozyrev, A.; Mohammad, A.; Rodgers, M. A. J.; Smith, K. M.; Dougherty, T. J. *J. Med. Chem.* **1997**, *40*, 3770.

(13) (a) Pandey, R. K.; Sumlin, A. B.; Potter, W. R.; Bellnier, D. A.; Henderson, B. W.; Constantine, S.; Apodia, M.; Rodgers, M. R.; Smith, K. M.; Dougherty, T. J. *Photochem. Photobiol.* **1996**, *63*, 194. (b) Henderson, B. W.; Bellnier, D. A.; Graco, W. R.; Sharma, A.; Pandey, R. K.; Vaughan, L.; Weishaupt, K. R.; Dougherty, T. J. *Cancer Res.* **1997**, *57*, 4000.

(14) (a) Zheng, G.; Potter, W. R.; Camacho, S. H.; Missert, J. R.; Wang, G.; Bellnier, D. A.; Henderson, B. W.; Rodgers, M. A. J.; Dougherty, T. J.; Pandey, R. K. *J. Med. Chem.* **2001**, *44*, 1540. (b) Zheng, G.; Aoudia, M.; Lee, D.; Rodgers, M. A.; Smith, K. M.; Dougherty, T. J.; Pandey, R. K. *J. Chem. Soc., Perkin Trans. 1* **2000**, 3113.

(15) Henderson, B. W.; Sumlin, A. B.; Owczarczak, B. L.; Dougherty, T. J. *J. Photochem. Photobiol.* **1991**, *10*, 303 and references therein.

(16) Linnanto, J.; Korppi-Tommola, J. *Phys. Chem. Chem. Phys.* **2000**, *2*, 4962.

(17) (a) Goutermann, M, In *The Porphyrins*; Dolphyin, D., Ed.; Academic Press: New York, 1978; Vol. 3, p 1. (b) Scherz, A.; Rosenbach-Belkin, V.; Fisher, J. R. E. In *Chlorophylls*; Scheer, H., Ed.; CRC Press: Boca Raton, FL, 1991; p 237. (c) Hanson, L. K. In *Chlorophylls*; Scheer, H., Ed.; CRC Press: Boca Raton, FL, 1991; p 993.

(18) Geskes, C.; Hartwich, G.; Scheer, H.; Mäntele, W.; Heinze, J. *J. Am. Chem. Soc.* **1995**, *117*, 7776.

(19) D'Souza, F.; Villard, A.; Van Caemelbecke, E.; Franzen, M.; Boschi, T.; Tagliatesta, P.; Kadish, K. M. *Inorg. Chem.* **1993**, *32*, 4042.

(20) Mäntele, W.; Wollenweber, A.; Rashwan, F.; Heinze, J.; Nabedryk, E.; Berger, G.; Breton, J. *Photochem. Photobiol.* **1988**, *47*, 451.

(21) (a) Fuhs, M.; Mössler, H.; Huber, M. *Magn. Reson. Chem.* **1997**, *35*, 566. (b) Mössler, H.; Wittenberg, M.; Niethammer, D.; Mudrassagam, R. K.; Kurreck, H.; Huber, M. *Magn. Reson. Chem.* **2000**, *38*, 67.

(22) Fajer, J.; Borg, D. C.; Forman, A.; Dolphin, D.; Felton, R. H. *J. Am. Chem. Soc.* **1973**, *95*, 2739.

(23) (a) Hamm, P.; Gray, K. A.; Oesterhelt, D.; Feick, R.; Scheer, H.; Zinth, W. *Biochim. Biophys. Acta* **1993**, *1142*, 99. (b) Holzapfel, W.; Finkele, U.; Kaiser, W.; Oesterhelt, D.; Scheer, H.; Stilz, H.; Zinth, W. *Proc. Natl. Acad. Sci. U.S.A.* **1990**, *87*, 5168.

(24) DeSimone, R. E.; Drago, R. S. *J. Am. Chem. Soc.* **1970**, *92*, 2343.

(25) Perrin, D. D.; Armarego, W. L. F. *Purification of Laboratory Chemicals*; Butterworth-Heinemann: Oxford, U.K., 1988.

(26) (a) Becke, A. D. *J. Chem. Phys.* **1993**, *98*, 5648. (b) Lee, C.; Yang, W.; Parr, R. G. *Phys. Rev. B* **1988**, *37*, 785.

(27) Hehre, W. J.; Radom, L.; Schleyer, P. v. R.; Pople, J. A. *Ab Initio Molecular Orbital Theory*; Wiley: New York, 1986.

(28) Frisch, M. J.; Trucks, G. W.; Schlegel, H. B.; Scuseria, G. E.; Robb, M. A.; Cheeseman, J. R.; Zakrzewski, V. G.; Montgomery, J. A., Jr.; Stratmann, R. E.; Burant, J. C.; Dapprich, S.; Millam, J. M.; Daniels, A. D.; Kudin, K. N.; Strain, M. C.; Farkas, O.; Tomasi, J.; Barone, V.; Cossi, M.; Cammi, R.; Mennucci, B.; Pomelli, C.; Adamo, C.; Clifford, S.; Ochterski, J.; Petersson, G. A.; Ayala, P. Y.; Cui, Q.; Morokuma, K.; Malick, D. K.; Rabuck, A. D.; Raghavachari, K.; Foresman, J. B.; Cioslowski, J.; Ortiz, J. V.; Stefanov, B. B.; Liu, G.; Liashenko, A.; Piskorz, P.; Komaromi, I.; Gomperts, R.; Martin, R. L.; Fox, D. J.; Keith, T.; Al-Laham, M. A.; Peng, C. Y.; Nanayakkara, A.; Gonzalez, C.; Challacombe, M.; Gill, P. M. W.; Johnson, B. G.; Chen, W.; Wong, M. W.; Andres, J. L.; Head-Gordon, M.; Replogle, E. S.; Pople, J. A. *Gaussian 98*, revision A.7; Gaussian, Inc.: Pittsburgh, PA, 1998.

(29) A much longer lifetime (15 ns) was also observed with a negligible portion at a prolonged time.

(30) Fukuzumi, S.; Suenobu, T.; Patz, M.; Hirasaka, T.; Itoh, S.; Fujitsuka, M.; Ito, O. *J. Am. Chem. Soc.* **1998**, *120*, 8060.

(31) Arbogast, J. W.; Darmanyan, A. P.; Chrostopher, P. D.; Foote, S.; Rubin, Y.; Diederich, F. N.; Alvarez, M. M.; Anz, S. J.; Whetten, R. L. *J. Phys. Chem.* **1991**, *95*, 11.

(32) Fuhrhop, J.-H.; Kadish, K. M.; Davis, D. G. *J. Am. Chem. Soc.* **1973**, *95*, 5140.

(33) Kadish, K. M.; Royal, G.; Van Caemelbecke, E.; Gueletti, L. Metalloporphyrins in Nonaqueous Media: Database of Redox Potentials. In *The Porphyrin Handbook*; Kadish, K. M., Smith, K. M., Guilard, R., Eds.; Academic Press: San Diego, 2000; Vol. 9, Chapter 59.

(34) Otten, H. A. *Photochem. Photobiol.* **1971**, *14*, 589.

(35) Although DFT calculations underestimate the HOMO−LUMO gap, the increase in the HOMO−LUMO gap with increasing degree of macrocycle conjugation is unmistakable.

(36) At prolonged reaction time, however, a new absorption due to the dehydrogenation product appeared at 709 nm, and its intensity increased with reaction time.

(37) Fukuzumi, S.; Nakanishi, I.; Tanaka, K.; Suenobu, T.; Tabard, A.; Guilard, R.; Van Caemelbecke, E.; Kadish, K. M. *J. Am. Chem. Soc.* **1999**, *121*, 785.

(38) Huber, M.; Fuhs, M. *Ber. Bunsen-Ges. Phys. Chem.* **1996**, *100*, 2057.

(39) Kavarnos, G, J.; Turro, N. J. *Chem. Rev.* **1986**, *86*, 401.